

Prediction and observation of defect-induced room-temperature ferromagnetism in halide perovskites

Zhiguo Sun¹, Bo Cai¹, Xi Chen^{1,†}, Wenxian Wei², Xiaoming Li¹, Dandan Yang¹, Cuifang Meng¹, Ye Wu¹, and Haibo Zeng^{1,†}

¹MIIT Key Laboratory of Advanced Display Materials and Devices, Institute of Optoelectronics & Nanomaterials, College of Materials Science and Engineering, Nanjing University of Science and Technology, Nanjing 210094, China

²Testing Center, Yangzhou University, Yangzhou 225009, China

Abstract: The possibility to induce a macroscopic magnetic moment in lead halide perovskites (LHPs), combined with their excellent optoelectronic properties, is of fundamental interest and has promising spintronic applications. However, these possibilities remain an open question in both theory and experiment. Here, theoretical and experimental studies are performed to explore ferromagnetic states in LHPs originated from lattice defects. First-principle calculations reveal that shallow-level Br vacancies in defective CsPbBr₃ can produce spin-splitting states and the coupling between them leads to a ferromagnetic ground state. Experimentally, ferromagnetism at 300 K is observed in room-temperature synthesized CsPbBr₃ nanocrystals, but is not observed in hot-injection prepared CsPbBr₃ quantum dots and in CsPbBr₃ single crystals, highlighting the significance played by vacancy defects. Furthermore, the ferromagnetism in the CsPbBr₃ nanocrystals can be enhanced fourfold with Ni²⁺ ion dopants, due to enhancement of the exchange coupling between magnetic polarons. Room-temperature ferromagnetism is also observed in other LHPs, which suggests that vacancy-induced ferromagnetism may be a universal feature of solution-processed LHPs, which is useful for future spintronic devices.

Key words: lead halide perovskites; magnetic nanocrystals; halogen vacancy defects; DFT calculations; magnetic polarons

Citation: Z G Sun, B Cai, X Chen, W X Wei, X M Li, Dandan Yang and A Yang, C F Meng, Y Wu, and H B Zeng, Prediction and observation of defect-induced room-temperature ferromagnetism in halide perovskites[J]. *J. Semicond.*, 2020, 41(12), 122501. <http://doi.org/10.1088/1674-4926/41/12/122501>

Supporting Information

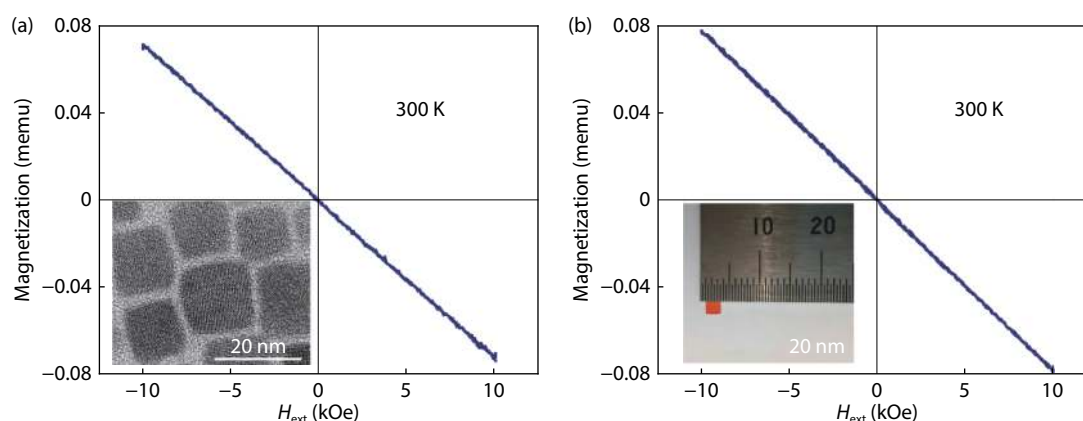


Fig. S1. (Color online) Magnetic properties of CsPbBr₃ quantum dots and single crystals. Pristine magnetization versus external magnetic field (H_{ext}) curves of (a) hot-injection synthesized CsPbBr₃ quantum dots and (b) CsPbBr₃ single crystals. Insets show corresponding sample morphology. Only linear diamagnetic background signals are observed in the two curves.

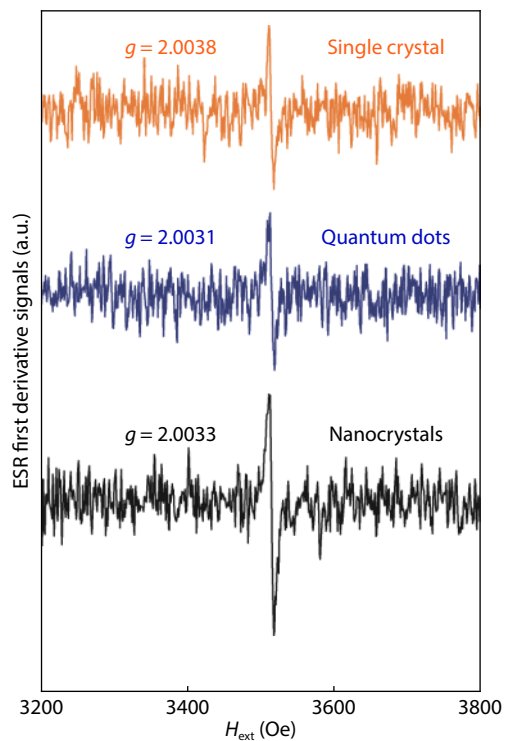


Fig. S2. (Color online) ESR characterization. First derivative of the ESR signals of room-temperature synthesized CsPbBr₃ nanocrystals, hot-injection synthesized CsPbBr₃ quantum dots, and CsPbBr₃ single crystals. These three samples had the same weight of 10.2 mg for the ESR measurement. The integrated resonance peak areas of the CsPbBr₃ quantum dots and the CsPbBr₃ single crystal were 50% smaller than that of the CsPbBr₃ nanocrystals, indicating a decrease of V_{Br} concentration in the former two samples.

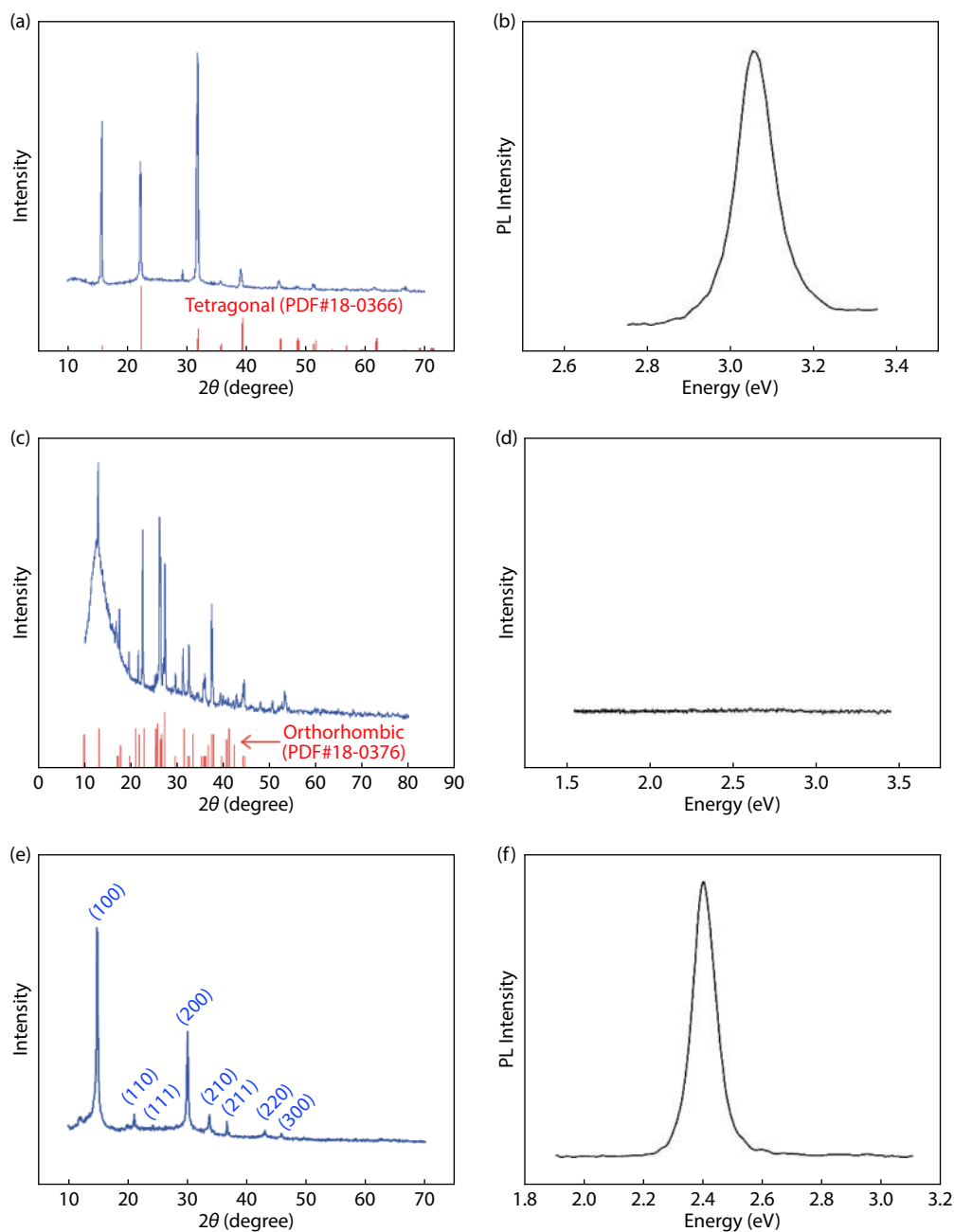


Fig. S3. (Color online) Structural and optical characterization of some LHPs. XRD patterns and photoluminescence (PL) spectra of room-temperature synthesized (a, b) CsPbCl_3 , (c, d) CsPbI_3 , and (e, f) $\text{CH}_3\text{NH}_3\text{PbBr}_3$. The CsPbCl_3 and CsPbI_3 were indexed as tetragonal (PDF#18-0366) and orthorhombic (PDF#18-0376)-phase structures, respectively. The $\text{CH}_3\text{NH}_3\text{PbBr}_3$ was found to have cubic-phase structures^[1]. The optical gaps of CsPbCl_3 and $\text{CH}_3\text{NH}_3\text{PbBr}_3$ were 3.05 and 2.39 eV, respectively. No emission was found in the PL spectrum of the orthorhombic-phase CsPbI_3 (also known as yellow-phase CsPbI_3), consistent with previous reports^[2]. All measurements were carried out at room temperature.

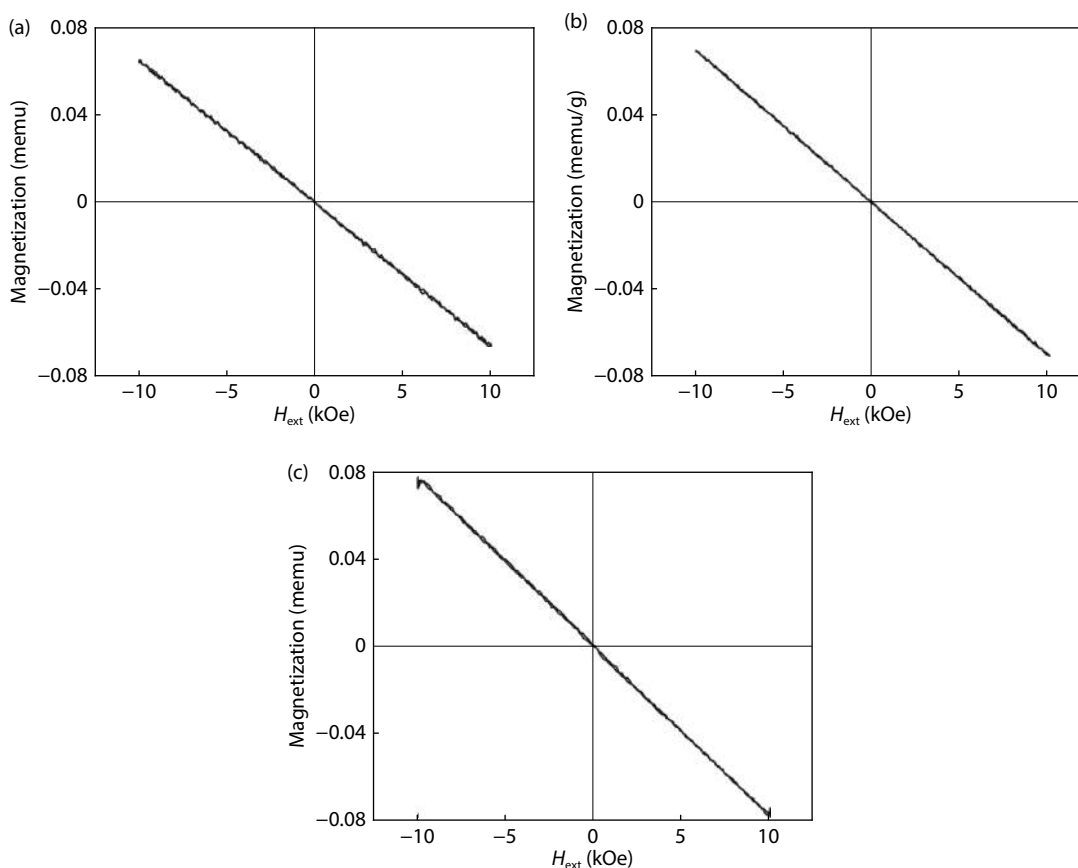


Fig. S4. Magnetic properties of hot-injection-synthesized LHPs. Pristine magnetization versus H_{ext} curves of (a) CsPbCl_3 , (b) CsPbI_3 , and (c) $\text{CH}_3\text{NH}_3\text{PbBr}_3$, measured at 300 K. Only linear diamagnetic background signals were observed in the three curves.

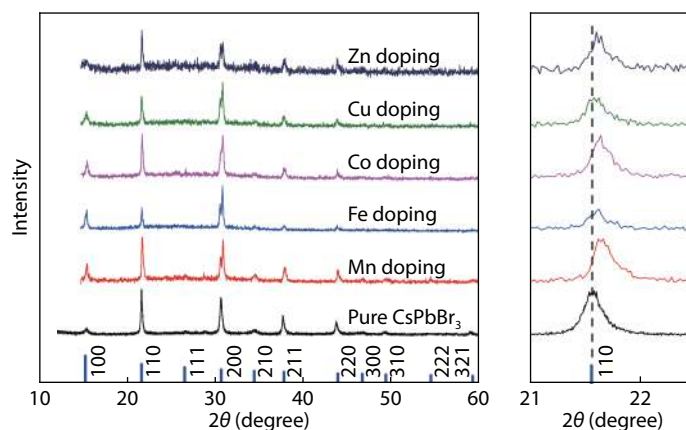


Fig. S5. XRD patterns of 3d ion-doped CsPbBr_3 synthesized at room temperature. The designed molar ratios of the Mn, Fe, Co, Cu, and Zn dopants, relative to Pb, were 15%. As shown in Table S1, the real molar ratio of the Mn, Fe, Co, Cu, and Zn relative to Pb were determined to be 1.7%, 0.54%, 0.87%, 0.35%, and 0.86%, respectively. The bottom blue vertical lines index the XRD patterns of CsPbBr_3 with a cubic-phase structure (PDF#54-0752). The Bragg angle, θ , shifts to a higher position after doping, indicating that the Mn, Fe, Co, Cu, and Zn dopants were successfully incorporated into the Pb sites.

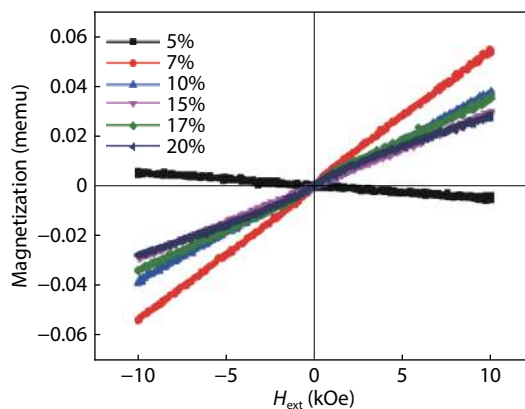


Fig. S6. (Color online) Magnetization curves of Ni-doped $\text{CsPb}_{1-y}\text{Ni}_y\text{Br}_3$ synthesized by hot injection. Here, y is the designed molar ratio of Ni relative to Pb. Only linear diamagnetic background signals were observed in the curve with $y = 5\%$. The curves with $y = 7\%$, 10% , 15% , 17% , and 20% showed paramagnetic behaviors. The measuring temperature was 300 K .

Table S1. Determination of dopant concentrations. Designed and real molar ratios of transition-metal (TM) ions relative to Pb ions in TM-doped CsPbBr_3 nanocrystals synthesized at room temperature. The real molar ratios were determined by inductively coupled plasma mass spectrometry.

TM dopant	Designed	Real
Ni	0%	0%
	5%	0.07%
	8%	0.09%
	10%	0.12%
	12%	0.22%
	15%	0.31%
	17%	0.42%
	20%	0.46%
Mn	15%	1.7%
Fe	15%	0.54%
Co	15%	0.87%
Cu	15%	0.35%
Zn	15%	0.86%

References

- [1] Kojima A, Teshima K, Shirai Y, et al. organometal halide perovskites as visible-light sensitizers for photovoltaic cells. *J Am Chem Soc*, 2009, 131(17), 6050
- [2] Ding X, Cai M, Liu X, et al. Enhancing the phase stability of inorganic $\alpha\text{-CsPbI}_3$ by the bication-conjugated organic molecule for efficient perovskite solar cells. *ACS Appl Mater Interfaces*, 2019, 11(41), 37720